Fast Forward-Backward Hankel Matrix Completion for Automotive Radar DOA Estimation Using Sparse Linear Arrays

Shunqiao Sun†, Yining Wen†, Ryan Wu‡, Dongyin Ren‡ and Jun Li‡

†Department of Electrical and Computer Engineering, The University of Alabama, Tuscaloosa, AL 35487
‡NXP Semiconductors, San Jose, CA 95134

***Abstract*—Automotive multiple-input multiple-output (MIMO) radar with sparse linear arrays is a cost-effective solution to achieve large aperture size with low hardware cost and reduced mutual coupling. The challenges associated with automotive MIMO sparse linear arrays are the high sidelobes, which might result in angular detection errors. This paper presents a fast forward-backward Hankel matrix completion and matrix pencil method for joint array interpolation and super-resolution single-snapshot angle finding by exploiting the structure of Hankel matrix. The novelty of the proposed approach lies in two parts. It not only saves the computational cost of singular value decomposition (SVD) in each iteration of the matrix completion, but also increases the degrees of freedom to construct a low-rank matrix with larger dimensions using the same number antenna elements, as a result of which, more targets can be completed and estimated with better accuracy. Numerical results demonstrate the effectiveness and efficiency of the proposed method.**

***Index Terms*—Sparse arrays, array interpolation, forward backward Hankel matrix, direction-of-arrival estimation, matrix pencil.**

I. Introduction

Millimeter wave (mmWave) radar can cope well with various weather and lighting conditions, and achieve reliable target perception at a lower cost than LiDAR. As a result, they are viewed as a key enabling technology to support autonomous driving [1]–[6]. Most automotive radar systems employ frequency-modulated continuous-wave (FMCW) transmit signals at the millimeter-wave band to achieve low-cost high-resolution sensing for complex functions during autonomous driving, such as automatic emergency braking, blind-spot detection, and adaptive cruise control [3].

Multiple-input multiple-output (MIMO) radar has been widely utilized in automotive radar design since it can synthesize a virtual array with large aperture size using a small number of transmit and receive antennas [7]–[9]. The aperture size can be further enlarged for automotive MIMO radar using sparse arrays [3], [10], [11]. Automotive radar with sparse arrays not only brings down the hardware cost but also reduces the mutual coupling among antennas [3]. The challenges associated with sparse arrays lie in the high sidelobes which may introduce angular ambiguity [12]. Interpolation techniques, such as linear regression [13], transform matrix [14]–[20], matrix completion [10], [11], [21], [22] or matrix reconstruction [23] approaches can be applied to interpolate the missing elements in the sparse arrays. Under the linear regression approach, usually a uniform linear subarray is needed to estimate the prediction coefficients first. For transform matrix approach, it usually works well for a narrow field of view (FOV) and thus a sector-based transform is required. Matrix completion approach provides flexibility in designing the sparse array geometries such that the missing elements can be filled by solving a low-rank matrix completion problem [10]–[12], [21], [22]. However, its computational cost is high due to the singular value decomposition (SVD) in each iteration. Fast algorithm, such as singular value thresholding (SVT) [24] has been developed. However, the structure of the Hankel matrix was not exploited in SVT.

It should be noted the difference coarray based sparse arrays, such as minimum redundancy array [25], nested array [26], coprime array [27], are popular in literature and they can resolve more number of targers than the number of physical array elements. However, these methods require a large number of array snapshots for accurate array covariance matrix estimation. In the highly dynamic scenario of autonomous driving, the number of array snapshots is often limited, and typically only a single snapshot is available [3].

In this paper, sum coarray i.e., MIMO radar, is considered for automotive radar, and only single-snapshot is avialble for direction-of-arrival (DOA) estimation. We propose a fast forward-backward (FB) Hankel matrix completion algorithm for array interpolation by exploiting the Hankel matrix structure. With the completed full array, angle finding is carried with matrix pencil approach [28], [29]. Our proposal achieves super-resolution in angle finding using only single snapshot of sparse arrays. The FB Hankel matrix approach has been proposed for super resolution spectrum estimation in [30]. However, the sparse array or sparse sampling was not considered there. We use only a small number of transmit and receive antennas to synthesize a large virtual sparse array via MIMO radar technology [3]. First, FB Hankel matrix

This work was supported in part by U.S. National Science Foundation (NSF) under Grant CCF-2153386 and Alabama Transportation Institute (ATI).

2023 IEEE Radar Conference (RadarConf23) | 978-1-6654-3669-4/23/$31.00 ©2023 IEEE | DOI: 10.1109/RADARCONF2351548.2023.10149466

completion based array interpolation not only smooths the noise effect on target's parameter estimation but also provides degree of freedom to construct a low-rank matrix with larger dimensions than the forward only (FO) case. As a result, more targets can be completed and estimated with better accuracy under FB. Second, the fast algorithm yields compact singular vectors of the completed FB Hankel matrix, which can be directly utilized in the matrix penci method. The proposal is evaluated via numerical simulations.

The rest of the paper is organized as follows. In Section II, we provide a review of the system model for forward-backward Hankel matrix completion based sparse array interpolation. Section III addresses the fast implementation of FB Hankel matrix completion and angle finding, while Section IV examines the numerical performance of the proposed method. Finally, we conclude the paper in Section V.

II. System Model

We consider a uniform linear array with M elements and half wavelength element spacing. Assume there are K targets with distinct angles $\{\theta_k\}, k = 1, \cdots, K$ in the same range-Doppler bin. With the noiseless forward only array response $\mathbf{y} = [y_1, y_2, \cdots, y_M]^T$, a Hankel matrix $\mathcal{H}(\mathbf{y})$ with dimensional of $M_1 \times L$ can be constructed as

$$\mathcal{H}(\mathbf{y}) = \begin{bmatrix} y_1 & y_2 & \cdots & y_L \\ y_2 & y_3 & \cdots & y_{L+1} \\ \vdots & \vdots & \ddots & \vdots \\ y_{M_1} & y_{M_1+1} & \cdots & y_M \end{bmatrix}, \tag{1}$$

where $M_1 = M - L + 1$. Here, L is the pencil parameter. The Hankel matrix $\mathcal{H}(\mathbf{y})$ has a Vandermonde decomposition [10], [31] structure

$$\mathcal{H}(\mathbf{y}) = \mathbf{A}\mathbf{\Sigma}\mathbf{B}^T, \tag{2}$$

where $\mathbf{A} = [\mathbf{a}(\theta_1), \cdots, \mathbf{a}(\theta_K)]$, $\mathbf{B} = [\mathbf{b}(\theta_1), \cdots, \mathbf{b}(\theta_K)]$ with

$$\mathbf{a}(\theta_k) = \left[1, e^{j2\pi\frac{d\sin(\theta_k)}{\lambda}}, \cdots, e^{j2\pi\frac{(M_1-1)d\sin(\theta_k)}{\lambda}}\right]^T, \tag{3}$$

$$\mathbf{b}(\theta_k) = \left[1, e^{j2\pi\frac{d\sin(\theta_k)}{\lambda}}, \cdots, e^{j2\pi\frac{(L-1)d\sin(\theta_k)}{\lambda}}\right]^T, \tag{4}$$

and $\mathbf{\Sigma} = \operatorname{diag}([\beta_1, \cdots, \beta_K])$. Thus, the rank of the Hankel matrix $\mathcal{H}(\mathbf{y})$ is K, assuming $M_1 > K$ and $L > K$. It is important to note that when selecting the pencil parameter L, it should be chosen in such a way that the resulting matrix $\mathcal{H}(\mathbf{y})$ is either a square matrix or an approximate square matrix. In that case, $L = \left\lfloor \frac{M+1}{2} \right\rfloor$, and the FO data matrix has dimension of $\left\lfloor \frac{M+1}{2} \right\rfloor \times \left\lfloor \frac{M+1}{2} \right\rfloor$.

The noiseless conjugate backward array response can be written as $\bar{\mathbf{y}} = [y_M^*, y_{M-1}^*, \cdots, y_1^*]^T$. Similarly, we can construct a Hankel matrix $\mathcal{H}(\bar{\mathbf{y}})$ with dimensional of $M_1 \times L$ using the backward array response. We can use the forward and backward Hankel matrices $\mathcal{H}(\mathbf{y})$ and $\mathcal{H}(\bar{\mathbf{y}})$ to formulate a block Hankel matrix $\mathbf{Y}_{FB} = \left[\begin{array}{cc} \mathcal{H}(\mathbf{y}) & \mathcal{H}(\bar{\mathbf{y}}) \end{array}\right] \in \mathbb{C}^{M_1 \times 2L}$. In the forward-backward case, the pencil parameter L should be adjusted such that the resulting matrix $\mathbf{Y}_{FB}$ is either a square matrix or an approximate square matrix. In that case, $L = \left\lfloor \frac{M+1}{3} \right\rfloor$, and the FB data matrix has dimension of $2\left\lfloor \frac{M+1}{3} \right\rfloor \times 2\left\lfloor \frac{M+1}{3} \right\rfloor$. We have the following Proposition regarding the rank of matrix $\mathbf{Y}_{FB}$.

Proposition 1. *The rank of the forward-backward block Hankel matrix* $\mathbf{Y}_{FB} = [\mathcal{H}(\mathbf{y}) | \mathcal{H}(\bar{\mathbf{y}})] \in \mathbb{C}^{M_1 \times 2L}$ *is* K *if* $M_1 > K$ *and* $L > K/2$.

Proof. See the proof in Appendix. □

The FB data matrix has a larger dimension than the FO data matrix while having the same rank. This results in more degrees of freedom (DOFs) for matrix completion. The additional DOFs in the FB data matrix offer several advantages. Firstly, sparse arrays with the same aperture but fewer antenna elements can be completed for the same number of targets. Secondly, for sparse arrays with the same aperture and the same number of antenna elements, a larger number of targets can be completed.

We consider a one-dimensional sparse array synthesized by MIMO radar technique [3]. By sparsely deploying M_t transmit and M_r receive antenna elements along horizontal direction on grid with grid size as half wavelength, we can synthesize a sparse linear array with $M_t M_r < M$ elements. The sparse virtual array has the same aperture as the full array. Let $\mathbf{y}_S \in \mathbb{C}^{M \times 1}$ denote the array response of the virtual sparse array, where the array response are filled with zeros at the $M - M_t M_r$ hole positions. Mathematically, $\mathbf{y}_S = \mathbf{y} \odot \mathbf{m}$, where $\odot$ denotes the Hadamard multiplication and $\mathbf{m} = [m_1, m_2, \cdots, m_M]^T$ is a mask vector with $m_j = 1$ if the j-th grid point is placed with a virtual array element or $m_j = 0$ if the j-th grid point is a hole. In practice, the array response is corrupted by additive white Gaussian noise with variance of σ^2, i.e.,

$$\mathbf{z}_S = \mathbf{y}_S + \mathbf{n}_S. \tag{5}$$

Let $\mathbf{Z}_{FB}^S = \left[\begin{array}{cc} \mathcal{H}(\mathbf{z}_S) & \mathcal{H}(\bar{\mathbf{z}}_S) \end{array}\right] \in \mathbb{C}^{M_1 \times 2L}$ denote the constructed block Hankel matrix, where $\bar{\mathbf{z}}_S = \bar{\mathbf{y}}_S + \bar{\mathbf{n}}_S$ is the conjugate backward of the noisy sparse array response $\mathbf{z}_S$. Here, $\bar{\mathbf{y}}_S = \bar{\mathbf{y}} \odot \bar{\mathbf{m}}$ and $\bar{\mathbf{m}}$ is a mask vector. To recover the holes in the sparse array, we aim to complete the low-rank forward-backward (FB) Hankel matrix. The noisy matrix completion is formulated as a rank minimization problem, defined below

$$\begin{aligned} &\min_{\mathbf{x}} \ \operatorname{rank}\left(\left[\begin{array}{cc} \mathcal{H}(\mathbf{x}) & \mathcal{H}(\bar{\mathbf{x}}) \end{array}\right]\right) \\ &\text{s.t.} \ \left\| \left[\begin{array}{cc} \mathcal{H}(\mathbf{x}) & \mathcal{H}(\bar{\mathbf{x}}) \end{array}\right] \odot \mathbf{M}_{FB} - \mathbf{Z}_{FB}^S \right\|_F \leq \delta. \end{aligned} \tag{6}$$

Here, $\mathbf{M}_{FB} = \left[\begin{array}{cc} \mathcal{H}(\mathbf{m}) & \mathcal{H}(\bar{\mathbf{m}}) \end{array}\right] \in \mathbb{R}^{M_1 \times 2L}$ is a mask matrix and $\delta = \sqrt{m + \sqrt{8m}\sigma}$ describes the noise bound with m being the number of nonzero entries of $\mathbf{M}_{FB}$.

III. Fast Forward-Backward Hankel Matrix Completion and DOA Estimation

We aim to develop an efficient iterative FB Hankel matrix completion algorithm without explicitly carrying out the singular value decomposition (SVD) of the FB Hankel matrix by exploiting its properties and structures. Based on the completed full array, the DOA estimation is carried out using the matrix pencil method.

A. Fast Forward-Backward Hankel Matrix Completion Using Iterative Hard Thresholding

The FB Hankel matrix recovery problem can be solved efficiently with iterative hard thresholding (IHT) method by exploiting the advantages of the Hankel structure [32]. In the n-th iteration, the new forward-backward array beamvectors $\mathbf{X}_n = \begin{bmatrix} \mathbf{x}_n & \bar{\mathbf{x}}_n \end{bmatrix} \in \mathbb{C}^{M\times 2}$ is updated as

$$\mathbf{X}_n = \mathbf{X}_{n-1} - \alpha_n \mathbf{D}_{n-1}, \tag{7}$$

where $\alpha_n = \frac{1}{\sqrt{n}}$ is the step size, and $\mathbf{D}_{n-1} \in \mathbb{C}^{M\times 2}$ is the sub-gradient, defined as

$$\mathbf{D}_{n-1} = \begin{bmatrix} \mathbf{z}_S & \bar{\mathbf{z}}_S \end{bmatrix} - \mathbf{X}_{n-1} \odot \begin{bmatrix} \mathbf{m} & \bar{\mathbf{m}} \end{bmatrix}. \tag{8}$$

In the n-th iteration, the obtained FB Hankel matrix $\mathbf{H}_n = \begin{bmatrix} \mathcal{H}(\mathbf{x}_n) & \mathcal{H}(\bar{\mathbf{x}}_n) \end{bmatrix} = \mathbf{U}_n \mathbf{\Sigma}_k \mathbf{V}_n^H$, with $\mathbf{U}_n \in \mathbb{C}^{M_1\times K}$ and $\mathbf{V}_n \in \mathbb{C}^{2L\times K}$, is first projected onto a tangent subspace $\mathbf{T}_n \in \mathbb{C}^{M_1\times 2L}$, which is defined as

$$\mathbf{T}_n = \{\mathbf{U}_n \mathbf{A}^H + \mathbf{B}\mathbf{V}_n^H | \mathbf{A} \in \mathbb{C}^{2L\times K}, \mathbf{B} \in \mathbb{C}^{M_1\times K}\}. \tag{9}$$

The projection can be rewritten as [33]

$$\mathcal{P}_{\mathbf{T}_n}\mathbf{H}_n = \begin{bmatrix} \mathbf{U}_n & \mathbf{Q}_2 \end{bmatrix} \mathbf{M}_n \begin{bmatrix} \mathbf{V}_n & \mathbf{Q}_1 \end{bmatrix}^H, \tag{10}$$

where

$$\mathbf{M}_n = \begin{bmatrix} \mathbf{U}_n^H \mathbf{H}_n \mathbf{V}_n & \mathbf{R}_1^H \\ \mathbf{R}_2 & \mathbf{0} \end{bmatrix} \in \mathbb{C}^{2K\times 2K}. \tag{11}$$

Here, $\mathbf{Q}_1 \in \mathbb{C}^{2L\times K}$ and $\mathbf{R}_1 \in \mathbb{C}^{K\times K}$ are from QR decompositions of the following matrix of dimensional $2L \times K$, with computational cost of $\mathcal{O}\left(2LK^2\right)$.

$$\left(\mathbf{I} - \mathbf{V}_n \mathbf{V}_n^H\right) \mathbf{H}_n^H \mathbf{U}_n = \mathbf{Q}_1 \mathbf{R}_1. \tag{12}$$

Similarly, $\mathbf{Q}_2 \in \mathbb{C}^{M_1\times K}$ and $\mathbf{R}_2 \in \mathbb{C}^{K\times K}$ are from QR decompositions of the following matrix of dimensional $M_1 \times K$, with computational cost of $\mathcal{O}\left(M_1 K^2\right)$.

$$\left(\mathbf{I} - \mathbf{U}_n \mathbf{U}_n^H\right) \mathbf{H}_n \mathbf{V}_n = \mathbf{Q}_2 \mathbf{R}_2. \tag{13}$$

In the above equations (12) and (13), the multiplications of $\mathbf{H}_n^H \mathbf{U}_n$ and $\mathbf{H}_n \mathbf{V}_n$ can be computed efficiently via fast Fourier transform (FFT) with computational cost of $\mathcal{O}(KM\log M)$ [34]. Let the reverse of the k-th column of the matrix $\mathbf{V}_n$ be $\overleftarrow{\mathbf{v}}_k = \mathrm{rev}(\mathbf{v}_k) = \left[\overleftarrow{\mathbf{v}}_{1k}, \overleftarrow{\mathbf{v}}_{2k}\right]^T \in \mathbb{C}^{2L\times 1}$. The multiplication of FB Hankel matrix with a vector is computed efficiently via FFT [34]

$$\mathbf{f} = \mathrm{ifft}\left[\mathrm{fft}\left(\mathrm{vec}\left(\mathbf{X}_n\right)\right) \odot \mathrm{fft}\left(\hat{\mathbf{v}}_k\right)\right], \tag{14}$$

where $\hat{\mathbf{v}}_k = \left[\overleftarrow{\mathbf{v}}_{1k}, \mathbf{0}, \overleftarrow{\mathbf{v}}_{2k}, \mathbf{0}\right]^T \in \mathbb{C}^{2M\times 1}$ is a zero-padding vector with $\mathbf{0}$ being a zero vector of length $M - L$. By extracting the last M_1 elements of $\mathbf{f}$, we have

$$\mathbf{H}_n \mathbf{v}_k = \mathrm{extract}\left(\mathbf{f}\right). \tag{15}$$

Then, FB Hankel matrix $\mathbf{H}_n$ is projected on to the set of rank K matrices.

$$\mathbf{H}_{n+1} = \mathcal{D}_K \mathcal{P}_{\mathbf{T}_n} \begin{bmatrix} \mathcal{H}(\mathbf{x}_n) & \mathcal{H}(\bar{\mathbf{x}}_n) \end{bmatrix} \tag{16}$$

where the hard thresholding operator $\mathcal{D}_K$ computes the rank K approximation via truncated SVD. The rank K truncated SVD of $\mathbf{M}_n \in \mathbb{C}^{2K\times 2K}$ can be represented as $\mathbf{M}_n = \mathbf{U}_M \mathbf{\Sigma}_M \mathbf{V}_M^H$ which can be computed in $\mathcal{O}\left(K^3\right)$ flops. Then the SVD of $\mathbf{H}_{n+1}$ can be written as

$$\mathbf{H}_{n+1} = \Bigg(\underbrace{\begin{bmatrix} \mathbf{U}_n & \mathbf{Q}_2 \end{bmatrix} \mathbf{U}_M}_{\mathbf{U}_{n+1}}\Bigg) \underbrace{\mathbf{\Sigma}_M}_{\mathbf{\Sigma}_{n+1}} \Bigg(\underbrace{\begin{bmatrix} \mathbf{V}_n & \mathbf{Q}_1 \end{bmatrix} \mathbf{V}_M}_{\mathbf{V}_{n+1}}\Bigg)^H$$

Finally, update the estimate of $\mathbf{X}_{n+1} = \begin{bmatrix} \mathbf{x}_{n+1} & \bar{\mathbf{x}}_{n+1} \end{bmatrix}$ as

$$\mathbf{x}_{n+1} = \sum_{k=1}^{K} \left[\mathbf{\Sigma}_{n+1}\right]_{k,k} \mathcal{H}^+ \left(\left[\mathbf{U}_{n+1}\right]_{:,k} \left(\left[\mathbf{V}_{n+1}\right]_{1:L,k}\right)^H\right) \tag{17}$$

$$\bar{\mathbf{x}}_{n+1} = \sum_{k=1}^{K} \left[\mathbf{\Sigma}_{n+1}\right]_{k,k} \mathcal{H}^+ \left(\left[\mathbf{U}_{n+1}\right]_{:,k} \left(\left[\mathbf{V}_{n+1}\right]_{L+1:2L,k}\right)^H\right) \tag{18}$$

where $\mathcal{H}^+$ denotes the left inverse of $\mathcal{H}$, i.e.,

$$\left[\mathcal{H}^+ \left(\left[\mathbf{U}_{n+1}\right]_{:,k} \left(\left[\mathbf{V}_{n+1}\right]_{1:L,k}\right)^H\right)\right]_t = \frac{1}{\rho_t} \sum_{a+b=t} \left[\mathbf{U}_{n+1}\right]_{a,k} \left[\mathbf{V}_{n+1}\right]_{b,k}^*,$$

$$\left[\mathcal{H}^+ \left(\left[\mathbf{U}_{n+1}\right]_{:,k} \left(\left[\mathbf{V}_{n+1}\right]_{L+1:2L,k}\right)^H\right)\right]_t = \frac{1}{\rho_t} \sum_{a+b=t} \left[\mathbf{U}_{n+1}\right]_{a,k} \left[\mathbf{V}_{n+1}\right]_{L+b,k}^*,$$

where ρ_t denotes the number of entries on the t-th anti-diagonal of $\mathcal{H}(\mathbf{x}_{n+1})$ or $\mathcal{H}(\bar{\mathbf{x}}_{n+1})$. It can be computed efficiently via fast convolution with computational cost of $\mathcal{O}(KM\log M)$.

The initialization of the fast sparse array interpolation algorithm is carried out via the Lanczos algorithm to obtain the $\mathbf{U}_0$ and $\mathbf{V}_0$ in $\mathcal{O}\left(M^2\right)$ [34]. Again the multiplication of the block Hankel matrix with a vector involved in the Lanczos algorithm can be computed efficiently via FFT with cost of $\mathcal{O}(KM\log M)$. The computational cost in each iteration is $\mathcal{O}\left(K^2M + KM\log M + K^3\right)$. The storage complexity of the fast algorithm is $\mathcal{O}(KM)$ since only the forward-backward beamvectors and corresponding SVD components need to be stored, while there is no need to express the block Hankel matrix explicitly.

The fast block Hankel matrix completion algorithm is summarized in Algorithm 1.

Algorithm 1 Sparse Array Interpolation via Fast Block Hankel Matrix Completion

Input: $\left[\begin{array}{cc}\mathbf{z}_S & \bar{\mathbf{z}}_S\end{array}\right]$: sparse forward-backward beamvectors corrupted with noise; K : model order; ϵ : precision level.

initialization: Find $\mathbf{U}_0$ and $\mathbf{V}_0$ of $\mathbf{Z}_{FB}^S$ via the Lanczos algorithm; obtain $\mathbf{x}_0$ and $\bar{\mathbf{x}}_0$ via (17) and (18); set $n=1$

while $\frac{\left\|\left[\begin{array}{cc}\mathbf{z}_S & \bar{\mathbf{z}}_S\end{array}\right]-\left[\begin{array}{cc}\mathbf{x}_n & \bar{\mathbf{x}}_n\end{array}\right]\odot\left[\begin{array}{cc}\mathbf{m} & \bar{\mathbf{m}}\end{array}\right]\right\|_F}{\left\|\left[\begin{array}{cc}\mathbf{z}_S & \bar{\mathbf{z}}_S\end{array}\right]\right\|_F} \geq \epsilon$ **do**

Calculate sub-gradient $\mathbf{D}_n = \left[\begin{array}{cc}\mathbf{z}_S & \bar{\mathbf{z}}_S\end{array}\right] - \mathbf{X}_n \odot \left[\begin{array}{cc}\mathbf{m} & \bar{\mathbf{m}}\end{array}\right]$

Update $\mathbf{X}_{n+1} = \mathbf{X}_n - \alpha_n \mathbf{D}_n$ with step size $\alpha_n = \frac{1}{\sqrt{n}}$

Calculate truncated SVD of $\mathbf{H}_{n+1}$ by updating

$$\begin{aligned}\mathbf{U}_{n+1} &= \left[\begin{array}{cc}\mathbf{U}_n & \mathbf{Q}_2\end{array}\right]\mathbf{U}_M\\ \mathbf{V}_{n+1} &= \left[\begin{array}{cc}\mathbf{V}_n & \mathbf{Q}_1\end{array}\right]\mathbf{V}_M\\ \mathbf{\Sigma}_{n+1} &= \mathbf{\Sigma}_M\end{aligned}$$

Obtain $\mathbf{X}_{n+1} = \left[\begin{array}{cc}\mathbf{x}_{n+1} & \bar{\mathbf{x}}_{n+1}\end{array}\right]$ via (17) and (18)

$n = n+1$

end while

Output : $\left[\begin{array}{cc}\mathbf{x}_{n+1} & \bar{\mathbf{x}}_{n+1}\end{array}\right]$ and $\mathbf{U}_{n+1}$

B. DOA Estimation via Forward-Backward Matrix Pencil Method

The DOA estimation is carried out using the forward-backward matrix pencil method (FBMPM) [29]. Let $\mathbf{Y}_{0FB}$ and $\mathbf{Y}_{1FB}$ be the matrices by deleting the last and first row of the block Hankel matrix $\mathbf{Y}_{FB}$, respectively. It holds that

$$\mathbf{Y}_{FB} = \left[\begin{array}{c}\mathbf{Y}_{0FB}\\ \mathbf{r}_{M_1}\end{array}\right] = \left[\begin{array}{c}\mathbf{r}_1\\ \mathbf{Y}_{1FB}\end{array}\right], \tag{19}$$

where $\mathbf{r}_1$ and $\mathbf{r}_{M_1}$ represent the first and last row of matrix $\mathbf{Y}_{FB}$, respectively. It holds that

$$\mathbf{Y}_{0FB} = \mathbf{U}_f \mathbf{\Sigma} \mathbf{V}^H, \tag{20}$$

$$\mathbf{Y}_{1FB} = \mathbf{U}_l \mathbf{\Sigma} \mathbf{V}^H, \tag{21}$$

where $\mathbf{U}_f$ and $\mathbf{U}_l$ are obtained by deleting the last and first row of matrix $\mathbf{U}$ that is obtained from Algorithm 1, respectively.

Considering the matrix pencil $\mathbf{Y}_{1FB} - \xi \mathbf{Y}_{0FB}$ and right multiplying it with $\mathbf{Y}_{0FB}^{+}$, the eigenproblem is

$$\mathbf{q}^H \left(\mathbf{Y}_{1FB}\mathbf{Y}_{0FB}^{+} - \xi \mathbf{I}\right) = \mathbf{0}^H, \tag{22}$$

where $\mathbf{Y}_{0FB}^{+}$ is the Moore-Penrose pseudo inverse of $\mathbf{Y}_{0FB}$. The problem is equivalent to the general eigenproblem of dimension $K \times K$

$$\mathbf{q}^H \left(\mathbf{U}_l^H \mathbf{U}_f - \xi \mathbf{U}_f^H \mathbf{U}_f\right) = \mathbf{0}^H. \tag{23}$$

Let the K eigenvalues are expressed as $\xi_k = \mathrm{Re}\{\xi_k\} + j\mathrm{Im}\{\xi_k\}, k = 1, \cdots, K$. These eigenvalues are related to the spatial frequencies that are determined by the targets' angles θ_k, i.e., $\xi_k = e^{j2\pi\frac{d\sin(\theta_k)}{\lambda}}$. And the targets' angles can be obtained as

$$\theta_k = \arcsin\left(\frac{\lambda}{2\pi d}\arctan\left(\frac{\mathrm{Im}\{\xi_k\}}{\mathrm{Re}\{\xi_k\}}\right)\right). \tag{24}$$

In the matrix completion based FBMPM, the obtained matrix $\mathbf{U}$ from Algorithm 1 containing the K left singular vectors is used to solve the $K \times K$ dimensional general eigenproblem of (23). As a result, the singular value decomposition step can be avoided in the FBMPM.

IV. Numerical Results

Consider two automotive radar transceivers [10] with $M_t = 6$ transmit and $M_r = 8$ receive antennas, which are deployed along the horizontal directions (see Fig. 1). The synthesized sparse virtual array has aperture of 76λ and the angular resolution is $\Delta\theta = 0.67^\circ$.

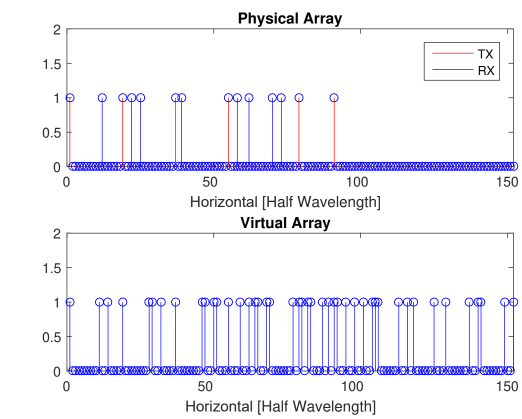

Fig. 1: Example of an automotive radar with virtual sparse array of 48 elements and aperture of 76λ.

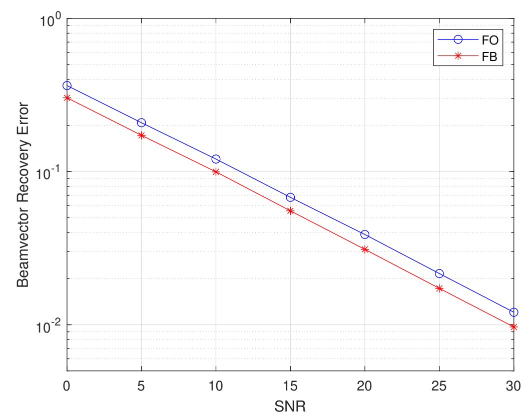

Fig. 2: Performance comparison between FO and FB: beamvector recovery errors decrease as SNR increases.

The performance comparison between forward only (FO) Hankel matrix completion and FB Hankel matrix completion is conducted. For the forward only case, the pencil parameter is chosen as $L = 76$ and the dimension of FO Hankel matrix is 76×76. For the FB case, the pencil parameter is chosen as $L = 51$ and the dimension of FB Hankel matrix is 102×102. Assume the recovered array response is denoted by $\hat{\mathbf{x}}$, corresponding to recovered backward backward array response as $\hat{\bar{\mathbf{x}}}$. The beamvector recovery error of FO and FB Hankel matrix are respectively defined as $\varepsilon_{FO} = \frac{\|\mathbf{y}-\hat{\mathbf{x}}\|}{\|\mathbf{y}\|}$ and $\varepsilon_{FB} = \frac{\left\|\left[\begin{array}{cc}\mathbf{y} & \bar{\mathbf{y}}\end{array}\right]-\left[\begin{array}{cc}\hat{\mathbf{x}} & \hat{\bar{\mathbf{x}}}\end{array}\right]\right\|_F}{\left\|\left[\begin{array}{cc}\mathbf{y} & \bar{\mathbf{y}}\end{array}\right]\right\|_F}$. We carried out independent runs in the Monte Carlo simulation. In the simulation, input signal-to-noise ratio (SNR) of $\mathbf{z}_S$ is set as $0, 5, 10, 15, 20, 25, 30$dB, respectively. For each SNR setting, the number of independent runs is set as $T = 1,000$. The noise is generated independently in each run, while the targets' angles at directions $\theta_1 = 10^\circ$ and $\theta_2 = 20^\circ$ and reflection coefficients are kept the same. It can be seen from Fig. 2 that both beamvector recovery errors decrease as the SNR increases, and the block Hankel matrix constructed with FB array response has a much lower recovery error than the FO scenario.

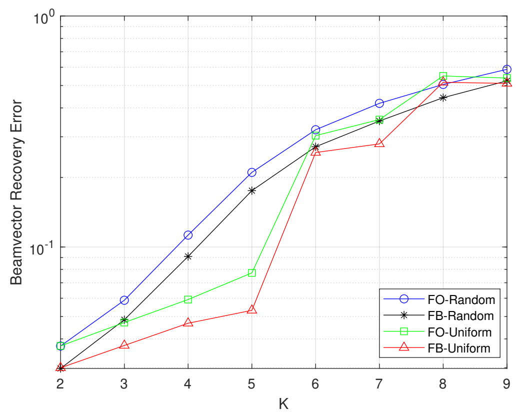

Fig. 3: Performance comparison between FO and FB: beamvector recovery errors increase as K increases.

We then test the beamvector recovery error as the number of targets increases when SNR = 20dB via Monte Carlo simulation for $T = 1,000$ independent runs. In each run, the targets are either uniformly or randomly chosen with minimum distance of $\Delta\theta$ in the field of view of $\left[-60^\circ, 60^\circ\right]$. The estimation is counted as a success if $\left|\hat{\theta}_k - \theta_k\right| < \Delta\theta/2$ for all the K targets. It can be seen from Fig. 3 and Fig. 4 that under both uniform and random of target distribution, the beamvector recovery error and estimation successful rate under FB have better performance than FO.

The dimension of the FB Hankel matrix is larger than the FO case, and thus more number of targets could be recovered successfully. To illustrate this advantage, we consider 5 targets with random angles. SNR is kept the same as 20dB. In Fig. 5, we plot the beampattern of recovered full array under both FO and FB approaches. It can be found that the peaks under FB are corresponding to ground truth obtained by full array,

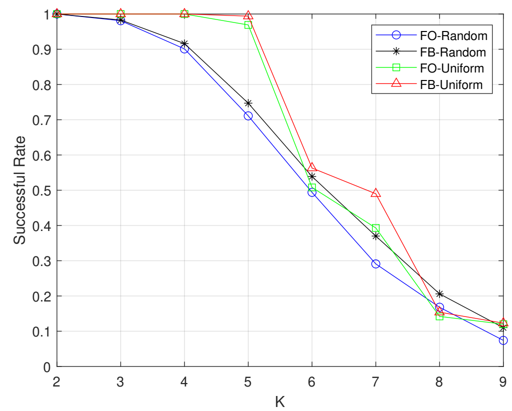

Fig. 4: Performance comparison between FO and FB: estimation successful rate decreases as K increases.

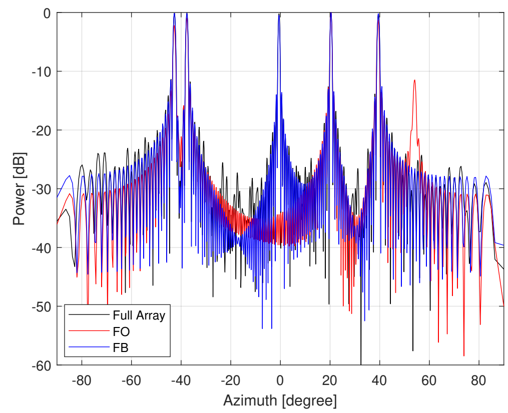

Fig. 5: Array beampatterns of 5 randomly generated target direction.

while there is false peak under FO approach.

V. Conclusions

We have demonstrated an automotive radar sparse array design approach using fast forward-backward Hankel matrix completion algorithm. By exploiting the structure in the Hankel matrix, it has been shown that it's not necessary to express the FB Hankel matrix explicitly during the SVD calculation, which saves both computation cost and storage space. Numerical simulations show the proposal has superior performance.

Appendix

The noiseless conjugate backward array response can be written as $\bar{\mathbf{y}} = \left[y_M^*, y_{M-1}^*, \cdots, y_1^*\right]^T$. Similarly, we can construct a Hankel matrix $\mathcal{H}\left(\bar{\mathbf{y}}\right)$ with dimensional of $M_1 \times L$ using the backward array response following equation (1). We show that the backward Hankel matrix $\mathcal{H}\left(\bar{\mathbf{y}}\right)$ can be written as

$$\mathcal{H}\left(\bar{\mathbf{y}}\right) = \mathbf{J}_{M_1}\mathbf{A}^*\mathbf{\Sigma}^*\mathbf{B}^H\mathbf{J}_L, \tag{25}$$

where $\mathbf{J}_{M_1}$ and $\mathbf{J}_L$ are exchange matrices, defined as

$$\mathbf{J}_{M_1} = \begin{bmatrix} 0 & & 1 \\ & \iddots & \\ 1 & & 0 \end{bmatrix}_{M_1 \times M_1}, \mathbf{J}_L = \begin{bmatrix} 0 & & 1 \\ & \iddots & \\ 1 & & 0 \end{bmatrix}_{L \times L}.$$

It holds that $\mathbf{J}_{M_1}\mathbf{A}^* = \mathbf{A}\mathbf{\Phi}^{-(M_1-1)}$ and $\mathbf{J}_L\mathbf{B}^* = \mathbf{B}\mathbf{\Phi}^{-(L-1)}$, where

$$\mathbf{\Phi} = \mathrm{diag}\left(\left[e^{j2\pi\frac{d\sin(\theta_1)}{\lambda}}, \cdots, e^{j2\pi\frac{d\sin(\theta_K)}{\lambda}}\right]\right). \tag{26}$$

The backward Hankel matrix $\mathcal{H}(\bar{\mathbf{y}})$ can be further written as

$$\begin{aligned}\mathcal{H}(\bar{\mathbf{y}}) =& \mathbf{J}_{M_1}\mathbf{A}^*\mathbf{\Sigma}^*\left(\mathbf{J}_L\mathbf{B}^*\right)^T \\ =& \mathbf{A}\mathbf{\Phi}^{-(M_1-1)}\mathbf{\Sigma}^*\left(\mathbf{B}\mathbf{\Phi}^{-(L-1)}\right)^T \\ =& \mathbf{A}\mathbf{\Phi}^{-(M_1-1)}\mathbf{\Sigma}^*\mathbf{\Phi}^{-(L-1)}\mathbf{B}^T \\ =& \mathbf{A}\mathbf{\Phi}^{-(M_1+L-2)}\mathbf{\Sigma}^*\mathbf{B}^T. \end{aligned} \tag{27}$$

In other words, the backward Hankel matrix $\mathcal{H}(\bar{\mathbf{y}})$ still enjoys a Vandermonde decomposition structure and its rank is K.

We can use the forward and backward Hankel matrices $\mathcal{H}(\mathbf{y})$ and $\mathcal{H}(\bar{\mathbf{y}})$ to formulate an enhanced Hankel matrix $\mathbf{Y}_{FB} = [\mathcal{H}(\mathbf{y})\,|\mathcal{H}(\bar{\mathbf{y}})] \in \mathbb{C}^{M_1 \times 2L}$, which can be written as

$$\begin{aligned}\mathbf{Y}_{FB} &= [\mathcal{H}(\mathbf{y})\,|\mathcal{H}(\bar{\mathbf{y}})] \\ &= \left[\mathbf{A}\mathbf{\Sigma}\mathbf{B}^T|\mathbf{A}\mathbf{\Phi}^{-(M_1+L-2)}\mathbf{\Sigma}^*\mathbf{B}^T\right] \\ &= [\mathbf{A}|\mathbf{A}]\begin{bmatrix}\mathbf{\Sigma} & \\ & \mathbf{\Phi}^{-(M_1+L-2)}\mathbf{\Sigma}^*\end{bmatrix}\begin{bmatrix}\mathbf{B} & \\ & \mathbf{B}\end{bmatrix}^T.\end{aligned}$$

It holds that $\mathrm{rank}\left([\mathbf{A}|\mathbf{A}]\right) = K$. Therefore, the rank of the enhanced Hankel matrix $\mathbf{Y}_{FB}$ is still K.

References

[1] S. Patole, M. Torlak, D. Wang, and M. Ali, "Automotive radars: A review of signal processing techniques," *IEEE Signal Process. Mag.*, vol. 34, no. 2, pp. 22–35, 2017.

[2] F. Engels, P. Heidenreich, A. M. Zoubir, F. K. Jondral, and M. Wintermantel, "Advances in automotive radar: A framework on computationally efficient high-resolution frequency estimation," *IEEE Signal Processing Magazine*, vol. 34, no. 2, pp. 36–46, 2017.

[3] S. Sun, A. P. Petropulu, and H. V. Poor, "MIMO radar for advanced driver-assistance systems and autonomous driving: Advantages and challenges," *IEEE Signal Process. Mag.*, vol. 37, no. 4, pp. 98–117, 2020.

[4] C. Waldschmidt, J. Hasch, and W. Menzel, "Automotive radar - From first efforts to future systems," *IEEE Journal of Microwaves*, vol. 1, no. 1, pp. 135–148, 2021.

[5] M. Markel, *Radar for Fully Autonomous Driving*. Boston, MA: Artech House, 2022.

[6] Z. Peng, C. Li, and F. Uysal, *Modern Radar for Automotive Applications*. London, UK: IET, 2022.

[7] J. Li and P. Stoica, "MIMO radar with colocated antennas," *IEEE Signal Process. Mag.*, vol. 24, no. 5, pp. 106–114, 2007.

[8] ——, *MIMO Radar Signal Processing*. Hoboken, NJ: Wiley, 2009.

[9] J. Bergin and J. R. Guerci, *MIMO Radar: Theory and Application*. Boston, MA: Artech House, 2018.

[10] S. Sun and Y. D. Zhang, "4D automotive radar sensing for autonomous vehicles: A sparsity-oriented approach," *IEEE J. Sel. Topics Signal Process.*, vol. 15, no. 4, pp. 879–891, 2021.

[11] ——, "Four-dimensional high-resolution automotive radar imaging exploiting joint sparse-frequency and sparse-array design," in *Proc. IEEE Int. Conf. Acoust., Speech, Signal Process. (ICASSP)*, Toronto, Canada, June 2021.

[12] S. Sun and A. P. Petropulu, "A sparse linear array approach in automotive radars using matrix completion," in *Proc. IEEE Int. Conf. Acoust., Speech, Signal Process. (ICASSP)*, Barcelona, Spain, May 2020.

[13] C. Alcalde and Z. Li, "Detector device including a shifted multi-dimensional array of detector elements," U.S. Patent 2018/0267143 A1, Sept. 20, 2018.

[14] B. Friedlander and A. J. Weiss, "Direction finding using spatial smoothing with interpolated arrays," *IEEE Trans. Aerosp. Electron. Syst.*, vol. 28, no. 2, pp. 574–587, 1992.

[15] ——, "Direction finding for wide-band signals using an interpolated array," *IEEE Trans. Signal Process.*, vol. 41, no. 4, pp. 1618–1634, 1993.

[16] P. Hyberg, M. Jansson, and B. Ottersten, "Array interpolation and bias reduction," *IEEE Trans. Signal Process.*, vol. 52, no. 10, pp. 2711–2720, 2002.

[17] ——, "Array interpolation and DOA MSE reduction," *IEEE Trans. Signal Process.*, vol. 53, no. 12, pp. 4464–4471, 2005.

[18] B. K. Lau, G. J. Cook, and Y. H. Leung, "An improved array interpolation approach to DOA estimation in correlated signal environments," in *Proc. IEEE Int. Conf. Acoust., Speech, Signal Process. (ICASSP)*, Montreal, Canada, May 2004.

[19] T. K. Yasar and T. E. Tuncer, "Wideband DOA estimation for nonuniform linear arrays with Wiener array interpolation," in *Proc. IEEE Workshop on Sensor Array and Multichannel Signal Processing (SAM)*, Darmstadt, Germany, July 2008.

[20] M. A. M. Marinho, J. Costa, F. Antreich, and L. Menezes, "Unscented transformation based array interpolation," in *Proc. IEEE Int. Conf. Acoust., Speech, Signal Process. (ICASSP)*, Brisbane, Australia, April 2015.

[21] S. Zhang, A. Ahmed, Y. D. Zhang, and S. Sun, "DOA estimation exploiting interpolated multi-frequency sparse array," in *Proc. IEEE Workshop on Sensor Array and Multichannel Signal Processing (SAM)*, Hangzhou, China, June 2020.

[22] ——, "Enhanced DOA estimation exploiting multi-frequency sparse array," *IEEE Trans. Signal Process.*, vol. 69, pp. 5935–5946, 2021.

[23] C. Zhou, Y. Gu, X. Fan, Z. Shi, G. Mao, and Y. D. Zhang, "Direction-of-arrival estimation for coprime array via virtual array interpolation," *IEEE Trans. Signal Process.*, vol. 66, no. 22, pp. 5956–5971, 2018.

[24] J. F. Cai, E. J. Candès, and Z. Shen, "A singular value thresholding algorithm for matrix completion," *SIAM J. Optim.*, vol. 20, no. 2, pp. 1956–1982, 2010.

[25] A. Moffet, "Minimum-redundancy linear arrays," *IEEE Trans. Antennas Propag.*, vol. 16, no. 2, pp. 172–175, 1968.

[26] P. Pal and P. P. Vaidyanathan, "Nested arrays: A novel approach to array processing with enhanced degrees of freedom," *IEEE Trans. Signal Process.*, vol. 58, no. 8, pp. 4167–4181, 2010.

[27] P. P. Vaidyanathan and P. Pal, "Sparse sensing with co-prime samplers and arrays," *IEEE Trans. Signal Process.*, vol. 59, no. 2, pp. 573–586, 2011.

[28] Y. Hua and T. K. Sarkar, "Matrix pencil method for estimating parameters of exponentially damped/undamped sinusoids in noise," *IEEE Trans. Acoust., Speech, Signal Process.*, vol. 38, no. 5, pp. 814–824, 1990.

[29] J. Rio and T. K. Sarkar, "Comparison between the matrix pencil method and the Fourier transform technique for high-resolution spectral estimation," *Digital Signal Processing*, vol. 6, pp. 108–125, 1996.

[30] Z. Yang and X. Wu, "Forward-backward Hankel matrix fitting for spectral super-resolution," in *European Signal Processing Conference (EUSIPCO)*, Amsterdam, Netherlands, Aug. 24-28, 2020.

[31] J. Ying, J. F. Cai, D. Guo, G. Tang, Z. Chen, and X. Qu, "Vandermonde factorization of Hankel matrix for complex exponential signal recovery-application in fast NMR spectroscopy," *IEEE Trans. Signal Process.*, vol. 66, no. 21, pp. 5520–5533, 2018.

[32] J. F. Cai, T. Wang, and K. Wei, "Fast and provable algorithms for spectrally sparse signal reconstruction via low-rank Hankel matrix completion," *Appl. Comput. Harmon. Anal.*, vol. 46, pp. 94–121, 2019.

[33] H. Cai, J. F. Cai, T. Wang, and G. Yin, "Accelerated structured alternating projections for robust spectrally sparse signal recovery," *IEEE Trans. Signal Process.*, vol. 69, pp. 809–821, 2021.

[34] L. Lu, W. Xu, and S. Qiao, "A fast SVD for multilevel block Hankel matrices with minimal memory storage," *Numerical Algorithms*, vol. 69, pp. 875–891, 2015.